Modulational Instability Induced by Cavity Boundary Conditions in a Normally Dispersive Optical Fiber

S. Coen and M. Haelterman

Service d'Optique et Acoustique, Université Libre de Bruxelles, 50 Av. F. D. Roosevelt, CP 194/5, B-1050 Bruxelles, Belgium

(Received 17 June 1997)

We study experimentally the role played by cavity boundary conditions in the onset of modulational instability in nonlinear and dispersive waves. This study is performed by means of an externally driven optical cavity made of a single-mode silica fiber. Spectral measurements of the intracavity field allow us to identify modulational instability in the presence of normal dispersion. This finding demonstrates that cavity boundary conditions fundamentally alter the physical mechanisms which are at the origin of modulational instability. [S0031-9007(97)04357-3]

PACS numbers: 42.65.Sf, 42.60.Da, 42.65.Re, 42.65.Wi

Modulational instability is a general feature of wave propagation in nonlinear dispersive media and is of common occurrence in such diverse fields as plasma physics [1], fluid dynamics [2], and nonlinear optics [3]. It refers to the physical process in which a weak periodic perturbation of a uniform intense carrier wave grows exponentially as a result of the interplay between dispersion and nonlinearity. In the field of nonlinear optics special attention has been paid to modulational instability in dispersive Kerr media (e.g., optical fibers) in which light-wave propagation is ruled by the nonlinear Schrödinger (NLS) equation [3]. In this context, nonlinear propagation phenomena are commonly described in terms of the parametric four-wave mixing processes which underlie them [3]. In particular, modulational instability arises in dispersive Kerr media because its underlying four-wave mixing process is naturally phase matched by the intensity-dependent refractive index. In self-focusing Kerr media, such as silica optical fibers, anomalous dispersion is required in order for this phase-matching process to occur. In the presence of normal dispersion, phase matching can be achieved only with the help of an extra degree of freedom that is provided by the coupling with an additional intense carrier wave of different polarization [4] or wavelength [5].

In 1992 Haelterman *et al.* suggested in a theoretical work that this extra coupling mechanism is not necessary to obtain an extension of the phenomenon of modulational instability to the normal dispersion regime [6]. It was shown that when nonlinear dispersive waves are subject to cavity boundary conditions, the underlying four-wave mixing processes are altered so as to make possible modulational instability with normal dispersion. The aim of the present Letter is to provide experimental evidence for this fundamental role of cavity boundary conditions in the onset of modulational instability. Since cavities are commonly encountered in nonlinear systems and since modulational instability is a ubiquitous phenomenon in nonlinear science, our observations are liable to be relevant to other fields of research such as plasma physics or fluid dynamics.

Our investigation of intracavity modulational instability has been performed with the all-fiber ring cavity depicted in Fig. 1. This type of device has already been studied experimentally by several authors with the aim of demonstrating and characterizing optical bistability, modulational instability, chaos, and turbulence [7–11]. Its principle of operation is the following: Light is launched into the cavity by means of a fiber coupler (C1). It then propagates along the fiber where it suffers the effects of the chromatic dispersion and the Kerr nonlinearity of silica. Besides these effects, the intracavity light wave undergoes cavity boundary conditions which manifest themselves by an attenuation due to the input coupler transmission and, more importantly, by a recurrent coherent superposition with the input beam (we neglect throughout the additional loss due to the output coupler C2). These four physical processes are mathematically described by the following infinite-dimensional map

$$E^{n+1}(0,t) = \sqrt{\rho}\, E^n(L,t)\, \exp(i\psi_0) + \sqrt{\theta}\, E_i\,, \quad (1)$$

$$\frac{\partial E^n(z,t)}{\partial z} = -i\,\frac{\beta_2}{2}\,\frac{\partial^2 E^n(z,t)}{\partial t^2} + i\gamma |E^n(z,t)|^2 E^n(z,t)\,, \quad (2)$$

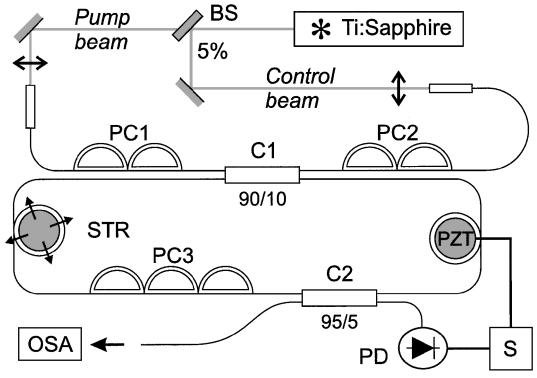

FIG. 1. Experimental setup. BS: 5% beam splitter; PC: polarization controller; STR: mechanical stretcher; PZT: piezoelectric stretcher; S: servo-control system; PD: photodetector; OSA: optical spectrum analyzer.

where $E^n(z,t)$ is the electric field envelope during the nth pass in the cavity, z is the longitudinal coordinate along the fiber axis, and t is the time in a reference frame traveling at the group velocity of light. The parameters ρ and θ are the intensity reflection and transmission coefficients of the input coupler on which a wave of amplitude E_i is launched ($\rho + \theta = 1$). L is the cavity length while ψ_0 is the linear phase shift acquired by the light wave over this length. β_2 and γ are, respectively, the group velocity dispersion and Kerr nonlinearity coefficients of the fiber.

The map, Eqs. (1) and (2), is similar to that introduced by McLaughlin *et al.* to study the dynamics of diffractive light beams in nonlinear ring cavities [12]. On the basis of analytical and numerical results, these authors showed that, when accounting for the transverse dimension of the light beams, the transition to chaos does not follow the scenario of period-doubling cascade predicted in the early work of Ikeda [13]. The reason for this is that complex spatial structures are generated through the combined action of diffraction and nonlinearity. Although they are due to a different phenomenology, our experimental observations are intimately linked to this theoretical prediction.

Let us now briefly consider the theory of intracavity modulational instability (MI). To this end we introduce the scaling $\xi = z/L$, $U^n = \sqrt{\gamma L}\,E^n$, $\tau = t/\sqrt{|\beta_2|L}$ so that the NLS equation (2) writes $U^n_\xi = -i(\eta/2)U^n_{\tau\tau} + i|U^n|^2U^n$, where η is the sign of dispersion, $\eta = \beta_2/|\beta_2|$. The instability against the growth of periodic perturbations of a steady-state continuous wave (cw), $U^n(\xi,\tau) = U_0\exp(i|U_0|^2\xi)$, propagating along the cavity fiber, is investigated by introducing, in the NLS equation, the ansatz $U^n(\xi,\tau) = [U_0 + v^n_1(\xi)\times\exp(i\Omega\tau) + v^n_{-1}(\xi)\exp(-i\Omega\tau)]\exp(i|U_0|^2\xi)$. At first order in the amplitudes of the Stokes waves $v^n_{\pm1}$, we obtain the linear problem $d\vec{v}^n/d\xi = M\vec{v}^n$, where $\vec{v}^n = (v^n_1, v^{n*}_{-1})^T$. Its general solution is $\vec{v}^n = (a^n, b^n)^T\exp(\mu\xi) + (c^n, d^n)^T\exp(-\mu\xi)$, where the eigenvector components satisfy the relation

$$a^n/b^n = d^n/c^n = -|U_0|^2/(|U_0|^2 + \eta\Omega^2/2 + i\mu), \tag{3}$$

and the eigenvalue μ writes

$$\mu = \Omega\sqrt{-\eta|U_0|^2 - \Omega^2/4}, \tag{4}$$

which provides the MI gain seen by the wave when propagating in the cavity fiber. This well-known result shows that the gain maximum is obtained for a modulation frequency of $\Omega_{\rm opt} = \sqrt{-2\eta|U_0|^2}$ which corresponds to phase matching of the underlying wave mixing process [3]. We see, in particular, that MI cannot occur in normally dispersive fibers, i.e., when $\eta = 1$.

We shall now see that the introduction of the cavity boundary conditions drastically alters this result. Since we follow a procedure similar to that of Ref. [12], we only give the main lines of the developments. Assuming that the incident wave amplitude E_i is constant, the cavity boundary conditions for the Stokes waves write

$$v^{n+1}_{\pm1}(\xi = 0) = \sqrt{\rho}\,\exp[i(\psi_0 + |U_0|^2)]\,v^n_{\pm1}(\xi = 1). \tag{5}$$

Expressing these relations in terms of the components a^n, b^n, c^n, d^n and using Eq. (3), we obtain an algebraic equation of the form $(a^{n+1}, c^{n+1})^T = Q(\rho, \psi_0, |U_0|^2, \eta\Omega^2)\,(a^n, c^n)^T$. When the modulus of at least one of the eigenvalues of the matrix Q is larger than unity, the Stokes waves undergo exponential growth during their multiple passes in the cavity. Since this matrix depends on the cavity parameters ρ and ψ_0 one can easily anticipate a strong influence of the cavity boundary conditions on MI.

The potentially unstable eigenvalues of Q are

$$q_\pm = \sqrt{\rho}\,(p \pm \sqrt{p^2 - 1}), \tag{6}$$

where $p = \cos(\phi)\cosh(\mu) - (|U_0|^2 + \eta\Omega^2/2)\sin(\phi)\times\sinh(\mu)/\mu$, with $\phi = \psi_0 + |U_0|^2$. For the sake of simplicity, we shall now restrict our analysis of intracavity MI to the good cavity limit; i.e., we assume that $\theta = 1 - \rho \approx O(1)$. In this limit, we can introduce the mean field approximation which implies, in the present context, that $|U_0|^2, \eta\Omega^2, \theta \approx O(1)$ [6]. Accordingly, the in-line MI gain μ given in Eq. (4) is also a quantity of order one. At first order, we have $p \approx \cos(\phi) - (|U_0|^2 + \eta\Omega^2/2)\sin(\phi)$ and from expression (6) of the intracavity MI gain, one can easily infer that the instability appears for values of ψ_0 close to a multiple of π, i.e., for the largest values of $|p|$. Practically, this means that MI occurs either close to cavity resonances $\psi_0 \approx 2m\pi$ or under antiresonant conditions $\psi_0 \approx (2m+1)\pi$. In the former (latter) case q_+ (q_-) is the corresponding unstable eigenvalue. This observation allows us to introduce a small detuning parameter $\delta \approx O(1)$ which measures the distance from resonance in one case, $\delta = 2m\pi - \psi_0$, and from antiresonance in the other, $\delta = (2m+1)\pi - \psi_0$. With this definition, we can simplify the eigenvalues, Eq. (6), by means of a first order expansion which yields

$$q_\pm = \pm\left[1 - \frac{\theta}{2} + \sqrt{4\left(\delta - \frac{\eta\Omega^2}{2}\right)|U_0|^2 - \left(\delta - \frac{\eta\Omega^2}{2}\right)^2 - 3|U_0|^4}\right], \tag{7}$$

where the sign + (−) refers to the resonant (antiresonant) condition. Equation (7) provides the MI gain, $G_{\rm MI} = |q_\pm| - 1$, characteristic of the exponential growth of the Stokes waves circulating in the cavity. This yields a MI gain spectrum identical to that derived in Ref. [6]. Note, however, that the negative eigenvalue in

Eq. (7), corresponding to antiresonant conditions, was not described in the analysis of Ref. [6]. This negative eigenvalue is important since it indicates that MI in antiresonant conditions manifests itself with a change of sign of the Stokes waves at each round trip. This behavior is reminiscent of period-doubling instabilities [12]. That is why, in order to differentiate the resonant and antiresonant MI regimes, we call them cw-MI and P2-MI, respectively.

The important result of this analysis is that it predicts the onset of MI in the normal dispersion regime. This can be easily seen by analyzing the gain spectrum Eq. (7) whose maximum is located in $\Omega_{\text{opt}} = \sqrt{2\eta(\delta - 2|U_0|^2)}$. It was shown in Ref. [6] for cw-MI that this relation corresponds to the phase-matching condition of the four-wave mixing process that underlies intracavity MI. We can therefore conclude that MI occurs in the normal dispersion regime ($\eta = 1$) owing to the role played by the cavity detuning in the phase-matching conditions.

To complete our theoretical description, we show in Fig. 2 an example of MI gain spectrum, $G_{\text{MI}} = |q_{\pm}| - 1$, as given from the exact expression Eq. (6). This spectrum consists of a series of peaks representing alternatively cw-MI and P2-MI. A good approximation of the optimal frequencies Ω_k corresponding to the peaks maxima is provided by their values in the good cavity limit

$$2|U_0|^2 + \eta\Omega_k^2/2 + \psi_0 = k\pi\,, \tag{8}$$

where even (odd) values of k correspond to cw-MI (P2-MI).

Experiment.—For obvious reasons of mathematical simplicity, the above theoretical developments are based on the stability analysis of a cw light beam. However, in practice, due to the weakness of the silica fiber nonlinearity, the input peak powers required to get modulational instability are much too high ($\simeq$ 1 kW) to allow for cw operation. Therefore, in our experiment (see Fig. 1) we used a mode-locked laser (Ti-sapphire) as input light source. This laser emits 1.25 ps sech-shaped pulses with a repetition rate of 82 MHz and a wavelength of 980 nm for which the fiber dispersion is $\beta_2 = 26$ ps^2/km. Average output powers of up to 1 W corresponding to 8 kW peak power can be achieved. In order to make our model Eqs. (1) and (2) valid with such a source, we must adjust the fiber length L so that, at each round trip, the intracavity pulse is superposed upon the input pulses. For technical reasons this synchronization has been achieved with $L = 7.38$ m which corresponds to 3 pulses per cavity round trip (the length adjustment is performed by means of a mechanical fiber stretcher, STR).

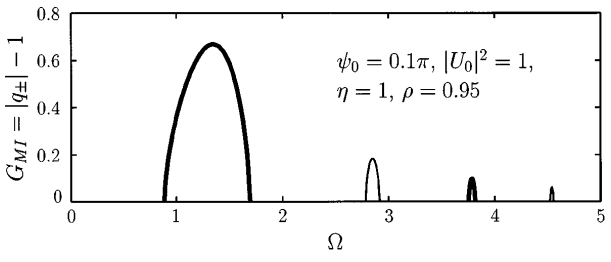

FIG. 2. MI gain spectrum: thin (bold) lines indicate cw-MI (P2-MI) sidelobes.

As discussed above, the theory predicts that the detuning plays a fundamental role in the dynamics of the cavity. The control of this parameter is therefore crucial for the experimental study of intracavity MI. We achieved accurate control of the cavity detuning by means of an interferometric stabilization scheme based on cavity polarization mode nondegeneracy. Its principle of operation is sketched in Fig. 1. A small fraction (5%) of the laser beam is deflected (by beam splitter BS) towards the second input port of the coupler C1. Since the intensity of this counterpropagating signal is low, the cavity behaves in its respect as a linear Fabry-Pérot resonator. Note that the nonlinear effects due to cross-phase modulation with the pump beam can be neglected due to the short duration of the pulses. The cavity can therefore be stabilized by tuning the fiber length in such a way that the counterpropagating signal is kept on resonance. This can be easily achieved by means of a servo-control device (S) that drives a piezoelectric fiber stretcher (PZT) on the basis of the resonator transmitted intensity measured through a photodetector (PD).

Since a fiber always exhibits residual birefringence, the cavity possesses in general two nondegenerate sets of resonances corresponding to orthogonal polarization eigenstates. The separation between the resonances of each polarization depends on the amount of birefringence. The use of polarization controllers at both cavity input ports (PC1 and PC2) allows us to pump the cavity along one polarization eigenstate with the nonlinear wave and along the orthogonal one with the linear control wave. In this situation, since the linear wave is kept on resonance, the cavity detuning δ seen by the nonlinear wave can be tuned by modifying the degree of birefringence through a third polarization controller inside the cavity (PC3). This system allows us to tune continuously the detuning parameter δ over a range of 2π with an accuracy estimated at 5%.

Owing to the excellent stability properties of our experimental setup, we have been able to comfortably study the spectra of the intracavity pulses by means of a high resolution optical spectrum analyzer (OSA). According to the above theory, when the power is sufficiently high, one must expect that the spectra appear as series of sideband peaks corresponding to the phase matching conditions Eq. (8). However, since the pulses we have at our disposal are short ($\sim$1 ps) as compared to typical MI oscillations ($\sim$1 THz), these phase-matching conditions cannot be merely applied by replacing $|U_0|^2$ by the pulse peak power. The value of the effective cw intensity that must be considered in Eq. (8) is of the order of the average pump intensity (i.e., the intensity of the cw component of the pump signal) and is naturally much lower. As a matter of fact, we have seen in

numerical simulations of the experiment that the positions of the sideband peaks exhibit only a very weak nonlinear dependence and that they can be well approximated by neglecting the contribution of the intensity in Eq. (8).

Figure 3(a) shows a typical example of MI spectrum. It is obtained with $\delta = 0.8\pi$ and an input peak power of 700 W (here δ refers to the distance from resonance, the distance from antiresonance being given by $\delta \pm \pi$). One clearly identifies a series of 4 symmetric sidebands. These sidebands are located in $f_0 = 0.82$ THz, $f_1 = 1.22$ THz, $f_2 = 1.53$ THz, and $f_3 = 1.78$ THz, as predicted by Eq. (8) which in real units writes $2\pi^2\beta_2 f_k^2 L - \delta \approx k\pi$. However, for even values of k the physical interpretation of the sideband peaks is ambiguous. Indeed, even in the linear regime, peaks can appear in the spectrum at the frequencies predicted by Eq. (8) with even values of k and when neglecting the cavity intensity. These peaks would simply correspond to the excitation of the closest resonances of the linear ring cavity. This excitation occurs when the spectrum of the cavity pulse is large enough to contain frequencies for which the dispersion phase-shift $2\pi^2\beta_2 f^2 L$ compensates for the detuning δ. This is what happens in our experiment due to the spectral broadening induced by self-phase modulation.

To the contrary, for odd values of k corresponding to P2-MI, the situation is unequivocal since the corresponding sidebands are located near antiresonant conditions for which the linear cavity transmission exhibits flat minima. The presence of sidebands at $f_1 = 1.22$ THz and $f_3 = 1.78$ THz constitutes therefore an irrefutable proof of the existence of the cavity-boundary-conditions-induced MI mechanism predicted theoretically. This interpretation is confirmed in Fig. 3(b) which shows the spectrum for the same detuning $\delta = 0.8\pi$ but with an input power lower than the MI threshold. As expected, the cavity resonances are still visible while the P2-MI peaks have completely vanished. Figure 3(c) shows the result of a numerical simulation of the experiment for the same parameter as those of Fig. 3(a) (i.e., with no fit parameter). Comparison with Fig. 3(a) reveals an excellent agreement between theory and experiment. The inset in Fig. 3(c) shows the modulated pulses emitted in the corresponding P2-MI regime, each pulse corresponding to half a period of the P2 cycle. Note that Fig. 3(c) is obtained by averaging the spectra of these two pulses, as is naturally performed in the experimental measurement. Similar numerical results have been reported by Vallée in Ref. [14] as regards both spectral and temporal behaviors.

In conclusion, we have demonstrated experimentally that cavity boundary conditions can drastically alter the basic physical mechanisms that are at the origin of modulational instability. This has been performed by providing evidence for the existence of modulational instability in a cavity made of a normally dispersive fiber. The simplicity of this device gives to our study a general character. Our conclusions are thus liable to be applied to other fields of nonlinear science and are important for the identification and understanding of the various complex spatiotemporal behaviors observed in practical systems.

This research was supported by the Fonds National de la Recherche Scientifique (Belgium) and the Inter-University Attraction Pole program of the Belgian government under Grant No. P4-07.

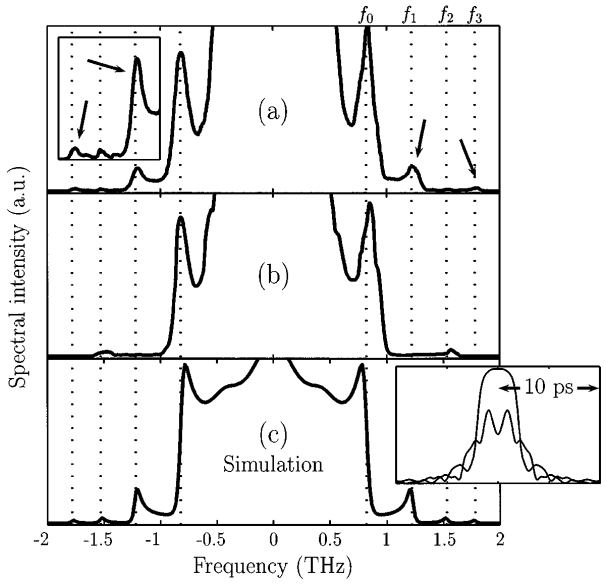

FIG. 3. Experimental pulse spectrum obtained for $\delta = 0.8\pi$ with input powers of (a) ~700 W (inset is a vertical zoom) and (b) ~450 W. Arrows indicate P2-MI sidelobes. (c) Numerical simulations of (a).

[1] A. Hasegawa, *Plasma Instabilities and Nonlinear Effects* (Springer-Verlag, Heidelberg, 1975).
[2] T. J. Benjamin and J. E. Feir, J. Fluid Mech. **27**, 417 (1967).
[3] G. P. Agrawal, *Nonlinear Fiber Optics* (Academic Press, San Diego, 1995).
[4] A. L. Berkhoer and V. E. Zakharov, Zh. Eksp. Teor. Fiz. **58**, 903 (1970) [Sov. Phys. JETP **31**, 486 (1970)].
[5] G. P. Agrawal, Phys. Rev. Lett. **59**, 880 (1987).
[6] M. Haelterman, S. Wabnitz, and S. Trillo, Opt. Lett. **17**, 745 (1992).
[7] H. Nakatsuka, S. Asaka, H. Itoh, K. Ikeda, and M. Matsuoka, Phys. Rev. Lett. **50**, 109 (1983).
[8] M. Nakazawa, K. Suzuki, and H. A. Haus, Phys. Rev. A **38**, 5193 (1988).
[9] R. Vallée, Opt. Commun. **81**, 419 (1991).
[10] M. B. van der Mark, J. M. Schins, and A. Lagendijk, Opt. Commun. **98**, 120 (1993).
[11] F. Mitschke, G. Steinmeyer, and A. Schwache, Physica (Amsterdam) **96D**, 251 (1996).
[12] D. W. McLaughlin, J. V. Moloney, and A. C. Newell, Phys. Rev. Lett. **54**, 681 (1985).
[13] K. Ikeda, Opt. Commun. **30**, 257 (1979).
[14] R. Vallée, Opt. Commun. **93**, 389 (1992).